JOURNAL OF VIROLOGY, Mar. 2007, p. 2349–2358 Vol. 81, No. 5
0022-538X/07/$08.00+0 doi:10.1128/JVI.01910-06

Tissue-Specific Regulation of CD8$^+$ T-Lymphocyte Immunodominance in Respiratory Syncytial Virus Infection$^\nabla$

Sujin Lee,[1,3] Scott A. Miller,[4] David W. Wright,[1,4] Michael T. Rock,[1] and James E. Crowe, Jr.[1,2,3]*

Departments of Pediatrics[1] and Microbiology and Immunology[2] and The Program for Vaccine Sciences,[3] Vanderbilt University Medical Center, and Department of Chemistry,[4] Vanderbilt University, Nashville, Tennessee 37232

Received 6 September 2006/Accepted 5 December 2006

Cytotoxic T lymphocytes (CTLs) are critical for control of respiratory syncytial virus (RSV) infection in humans and mice. To investigate cellular immune responses to infection, it is important to identify major histocompatibility complex (MHC) class I-restricted CTL epitopes. In this study, we identified a new RSV-specific, H-2K^d-restricted subdominant epitope in the M2 protein, M2$_{127\text{-}135}$ (amino acids 127 to 135). This finding allowed us to study the frequency of T lymphocytes responding to two H-2K^d-presented epitopes in the same protein following RSV infection by enzyme-linked immunospot (ELISPOT) and intracellular cytokine assays for both lymphoid and nonlymphoid tissues. For the subdominant epitope, we identified an optimal nine-amino-acid peptide, VYNTVISYI, which contained an H-2K^d consensus sequence with Y at position 2 and I at position 9. In addition, an MHC class I stabilization assay using TAP-2-deficient RMA-S cells transfected with K^d or L^d indicated that the epitope was presented by K^d. The ratios of T lymphocytes during the peak CTL response to RSV infection that were specific for M2$_{82\text{-}90}$ (dominant) to T lymphocytes specific for M2$_{127\text{-}135}$ (subdominant) were approximately 3:1 in the spleen and 10:1 in the lung. These ratios were observed consistently in primary or secondary infection by the ELISPOT assay and in secondary infection by MHC/peptide tetramer staining. The number of antigen-specific T lymphocytes dropped in the 6 weeks after infection; however, the proportions of T lymphocytes specific for the immunodominant and subdominant epitopes were maintained to a remarkable degree in a tissue-specific manner. These studies will facilitate investigation of the regulation of immunodominance of RSV-specific CTL epitopes.

Respiratory syncytial virus (RSV) is the most common cause of serious viral lower respiratory tract illness in infants and young children (12, 14, 15, 28). Cytotoxic T lymphocytes (CTLs) provide an essential component of the immune response to most viral infections, and CD8$^+$ CTLs contribute to the resolution of RSV infection (17). CTLs use the T-cell receptor to recognize small antigenic peptides that are associated with major histocompatibility complex (MHC) class I molecules. RSV proteins that have been previously shown to induce CTL activity in humans include the nucleoprotein, the fusion (F) protein, the matrix 2 open reading frame 1 (M2-1) protein, and the short hydrophobic protein (11, 34, 42). RSV proteins, including the nucleoprotein, F protein, and M2-1, also have been shown previously to induce CTL activity in mice (3, 8, 29). To date, four RSV-specific CTL epitopes for BALB/c mice have been identified, and one epitope for C57BL/6 mice has been identified (8, 19, 36, 41).

Previous studies defined an RSV CTL epitope for BALB/c mice in the M2 protein that dominates the T-cell response to the virus following primary infection and contributes to functional immunity that resolves the infection (21, 22). The immunodominant peptide SYIGSINNI, located at amino acid positions 82 to 90 in the protein, contains the consensus sequence for nonameric H-2K^d-restricted T-cell epitopes that specifies a Tyr residue at position 2 and a Val, Ile, Thr, Ala, or Leu at position 9. The original screening study concluded that the M2$_{82\text{-}90}$ peptide (amino acids 82 to 90) is the sole determinant of cellular immunity induced in BALB/c mice by the M2 protein. Interestingly, three additional peptides in the M2 protein possess the consensus sequence for an H-2K^d-restricted T cell epitope, M2$_{26\text{-}34}$, M2$_{71\text{-}79}$, and M2$_{127\text{-}135}$ (shown in Table 1). Since CTL activity in response to these three peptides could not be detected by using the relatively insensitive techniques available at the time of the original study (21), the investigators concluded that there is a single CTL epitope for BALB/c mice in the M2 protein. There is considerable interest in the role and influence of immunodominant CTL responses on the breadth and magnitude of other CTL responses to RSV; therefore, we sought to identify additional less-dominant epitopes for study in this model. Previous efforts to identify additional epitopes in RSV focused on proteins other than M2, such as the G (glycosylated or attachment) or F proteins.

We hypothesized that the M2 protein may contain another functional CTL epitope for BALB/c mice based on the previous findings (21, 22). In studies of protection induced by a vaccinia virus expressing a mutant RSV M2 protein containing a Y83R point mutation in the anchor residue of the M2$_{82\text{-}90}$ epitope, the percent RSV-specific lysis caused by T lymphocytes following inoculation was reduced to only 21%, compared to the 66% RSV-specific lysis induced by the unmutated M2 protein inoculation (21). The residual 21% specific lysis represents a reasonable level of killing activity and suggested that the M2 protein may contain one or more additional CTL epitopes. More-sensitive techniques for defining

* Corresponding author. Mailing address: T-2220 Medical Center North, 1161 21st Avenue South, Nashville, TN 37232-2905. Phone: (615) 343-8064. Fax: (615) 343-4456. E-mail: james.crowe@vanderbilt.edu.

$^\nabla$ Published ahead of print on 20 December 2006.

TABLE 1. Selected RSV M2 protein-derived peptides used in this study

Potential epitope designation[a]	M2 synthetic peptide	Peptide sequence[b]
$M2_{26-34}$	6	CHFSHN**Y**FEWPPH**A**L
	7	HN**Y**FEWPPH**A**LLVRQ
$M2_{71-79}$	17	ELDRTEE**Y**ALGVVG**V**
	18	TEE**Y**ALGVVG**V**LESY
$M2_{82-90}$	20	VGVLES**Y**IGSINN**I**T
	21	ES**Y**IGSINN**I**TKQSA
$M2_{127-135}$	31	NSPKIRV**Y**NTVISY**I**
	32	IRV**Y**NTVISY**I**ESNR

[a] Four regions in the M2 protein possess the consensus sequence for an H-2K^d-restricted epitope.

[b] The predicted 9 amino acid potential H-2K^d-restricted epitope is underlined; the full 15-amino-acid peptide tested experimentally is shown. The predicted anchor residues at position 2 (Y) or position 9 (A, V, or I) are in bold.

CTL epitopes, such as gamma interferon (IFN-γ) enzyme-linked immunospot (ELISPOT) assays, intracellular cytokine staining (ICS) assays for IFN-γ, and algorithm prediction programs for MHC binding of peptides, are now available. We sought to use this new set of tools to identify a subdominant epitope in M2.

There is a hierarchy in the epitope specificity of MHC class I-restricted responses to microbial pathogens in different experimental systems (1, 23, 37, 40, 43). The T-lymphocyte response to pathogens generally focuses on a small number of epitopes in murine models of infection. Immunodominant epitopes generate vigorous responses, and those eliciting smaller responses are considered subdominant (7). Various factors contribute to the dominance or subdominance of an epitope, such as (i) the efficiency of intracellular processing of the antigenic peptide, (ii) the binding affinity of the peptide for MHC class I, (iii) dominant CTL suppression of the development of subdominant responses via IFN-γ (35), and (iv) the T-cell receptor (TCR) repertoire available to respond to the MHC/peptide complex (9, 46).

In this study, we identified a novel RSV-specific, H-2K^d-restricted subdominant epitope in the M2-1 protein, $M2_{127-135}$, and we determined the frequency of T lymphocytes responding to the two epitopes presented by H-2K^d following RSV infection in lymphoid or nonlymphoid tissues and during primary or secondary infection. A comparison of the responses to these two epitopes allowed us to explore the regulation of immunodominance to an acute infection at early or late time points. We found that, although the absolute number of lymphocytes specific for each of these epitopes drops significantly in the weeks following immunization, the proportions of T lymphocytes directed to these two epitopes are highly regulated over time. Interestingly, the regulation of immunodominance in the site of infection differed from that in the systemic compartment.

MATERIALS AND METHODS

Mice. Respiratory-pathogen-free 6- to 8-week-old female BALB/c (H-2^d) mice were purchased from Harlan Sprague-Dawley Laboratory (Indianapolis, IN). We adhered to the *Guide for the Care and Use of Laboratory Animals* of the Committee on Care and Use of Laboratory Animals of the Institute of Laboratory Animal Resources, National Research Council, in conducting the research described in this paper (27a). All experiments were reviewed and approved by the Vanderbilt Institutional Animal Care and Use Committee. Animals were maintained in microisolator cages throughout the studies. Six- to eight-week-old pathogen-free female mice were anesthetized with inhaled methoxyflurane (Metofane; Pitman-Moore, Mundelein, IL) and immunized intranasally once (primary infection, day 0) or twice (secondary infection, day 0 and day 21) with 10^6 PFU of RSV in a 100-μl volume.

Synthetic peptides. A panel of 46 synthetic peptides that spans the complete RSV M2-1 protein of the RSV A2 strain was generated. M2-1 peptides were 15 amino acids in length, overlapping by 11 amino acids (purchased from Synpep Corporation, Dublin, CA). An H-2K^d-restricted peptide from influenza virus nucleoprotein ($NP_{147-155}$) and a cytomegalovirus peptide (pp89) were used as controls. Additional peptides were synthesized on single substituted 2-chlorotrityl resins (Synpep and Advanced Chemtech) in an Advanced Chemtech Apex 396 DC automated peptide synthesizer using a standard 9-fluorenylmethoxycarbonyl and *tert*-butyl protection scheme. Matrix assisted laser desorption ionization mass spectrometry with time of flight detector, electrospray ionization mass spectrometry, and amino acid analysis were used to confirm peptide identities. Purified peptides were lyophilized (Labconco Freezezone 4.5) and stored at −40°C until use. The peptides were synthesized and high-performance liquid chromatography purified to more than 95% purity.

To identify candidates for the optimal peptide epitope within the reactive 15-amino-acid peptides, we used three separate computer algorithms, SYFPEITHI (31), BIMAS (30), and RANKPEP (32, 33).

Cells and virus. HEp-2 cells (ATCC catalog no. CCL-23) were maintained in Opti-MEM I medium (Invitrogen) supplemented with glutamine, amphotericin B, gentamicin, and 2% fetal bovine serum (FBS). Wild-type strain A2 of RSV was grown in HEp-2 cell monolayer cultures, titrated, and stored in aliquots at −80°C until use as described previously (6).

Preparation of lung-derived lymphocytes and splenocytes. Mice were sacrificed by CO_2 inhalation at various time points, as indicated in the figures. The lung and spleen were removed and placed separately into complete RPMI supplemented with 10% FBS, L-glutamine, 2-mercaptoethanol, HEPES, and gentamicin (designated R10 medium). The tissues were minced and ground through a sterile steel mesh to obtain a single-cell suspension. For splenocytes, cells were treated with red blood cell lysing buffer (Sigma-Aldrich, St. Louis, MO). For lung lymphocytes, cells were layered onto Lympholyte-M density gradient medium (Cedarlane, Ontario, Canada) and lung mononuclear cells were isolated by centrifugation at 1,000 × *g*. Cells were counted and resuspended at the stated cell concentration for the appropriate in vitro assay.

ELISPOT assay. The IFN-γ ELISPOT assay was performed as previously described (2, 26), except for slight modifications. Briefly, 96-well plates (ELIP10SSP; Millipore, Bedford, MA) were coated with 10 μg/ml of anti-IFN-γ monoclonal antibody (MAb) (clone A18; Mabtech, Stockholm, Sweden) in phosphate-buffered saline (PBS) at 4°C overnight. Plates then were washed with sterile PBS three times and blocked with 10% RPMI for at least 2 h at room temperature. Peptides were added directly to wells in a volume of 50 μl, and then freshly isolated splenocytes were added at a concentration of 10^5 cells/well in 50 μl of R10 medium. The final concentration of the peptides in the screening assay was 10 μM. The plates were incubated for 18 to 20 h at 37°C in 5% CO_2. The plates were then washed, labeled with 2 μg/ml biotinylated anti-IFN-γ monoclonal antibody (clone R4-6A2; Mabtech) in PBS, and incubated at room temperature for 3 h. After additional washes, avidin-peroxidase complex (Vector Laboratories, Burlingame, CA) was added to each well in PBS for 1 h at room temperature. The plates were washed, and IFN-γ-producing cells were detected after a 4-min color reaction using 100 μl of AEC substrate (20 mg of 3-amino-9-ethylcarbazol; Sigma-Aldrich) dissolved in 2.5 ml of dimethylformamide, diluted 1:20 in 47.5 ml of sodium acetate buffer plus 25 μl 30% H_2O_2. IFN-γ-producing cells were counted by using an automated ELISPOT reader system and ImmunoSpot 3 software (Cellular Technology Ltd., Cleveland, OH). Results were expressed as the numbers of spot-forming cells (SFC) per 10^6 input cells.

ICS assay. To enumerate the IFN-γ-producing cells, intracellular staining was performed as previously described (27). In brief, freshly isolated splenocytes (2×10^6) were left untreated or stimulated with individual peptides (1 μg/sample) and costimulatory monoclonal antibodies anti-CD28 and anti-CD49d for 6 h at 37°C in 5% CO_2 in the presence of brefeldin A (10 μg/ml; Sigma). Cell surface staining was performed, followed by intracellular cytokine staining using the Cytofix/Cytoperm kit (BD Pharmingen, San Diego, CA) in accordance with the manufacturer's protocol. For tetramer analysis, freshly isolated cells (2×10^6) in R10 medium were incubated with pretitered, optimal amounts of H-2K^d M2 tetramers for 1 h on ice followed by surface staining for CD3, CD4, and CD8.

The following antibodies were obtained from BD Pharmingen: anti-CD3 fluorescein isothiocyanate, anti-CD4 phycoerythrin (PE)-Cy7, anti-CD8 Cy7-allophycocyanin, and anti-IFN-γ PE. Tetramers were obtained from Beckman Coulter. The

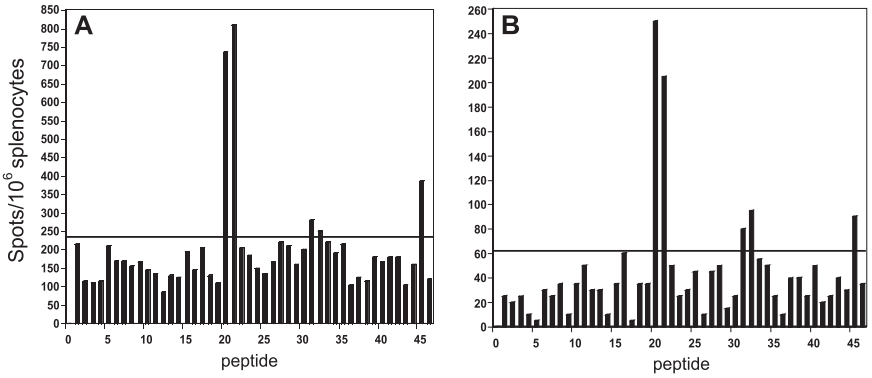

FIG. 1. Frequencies of RSV M2-1-specific IFN-γ-secreting mouse splenocytes after RSV immunization. A panel of peptides spanning the RSV M2 protein was tested for the ability of individual peptides to elicit IFN-γ production. At day 8 (acute) (A) or day 48 (memory) (B) after the second infection, mice were sacrificed and splenocytes were stimulated with 46 peptides individually. Data represent the results of a single experiment, which was one of three with similar results. A threshold of twice the average background value was used to identify peptides containing putative epitopes.

peptide epitopes used in these tetramers were SYIGSINNI ($M2_{82-90}$) and VYNTV ISYI ($M2_{127-135}$). Flow cytometry was performed using an LSRII cytometer (BD Immunocytometry Systems). Data analysis was performed using FlowJo software, version 6.1 (Tree Star, San Carlos, CA).

RMA-S stabilization assay. RMA-S cells expressing K^d were kindly provided by E. Pamer (Memorial Sloan Kettering Cancer Center, New York, NY), and RMA-S cells expressing L^d were kindly provided by T. Hansen (Washington University School of Medicine, St. Louis, MO). The RMA stabilization assay was performed as described previously (7). RMA-S cells were maintained in complete RPMI 1640 supplemented with 10% FBS, L-glutamine, 2-mercaptoethanol, HEPES, and gentamicin. RMA-S cells expressing K^d (10^6) and RMA-S cells expressing L^d (10^6) were maintained at 26°C for 18 to 24 h, pulsed with the indicated amounts of peptide in duplicate for 45 min at 26°C in a 5% CO_2 atmosphere, and transferred to 37°C for an additional 3 h. Cells were stained with biotinylated anti-K^d MAb (clone SF1-1,1; Pharmingen), or biotinylated anti-L^d MAb (clone 28-14-8; BioLegend, San Diego, CA) followed by PE-conjugated streptavidin (Pharmingen, San Jose), washed twice with fluorescence-activated cell sorter buffer, and analyzed by flow cytometry. The results were expressed as mean fluorescence intensity (MFI) ratios. The percent MFI increase was calculated as follows: percent MFI increase = (MFI with the given peptide − MFI without peptide)/(MFI without peptide) × 100.

RESULTS

Identification by ELISPOT of H-2^d-restricted 15-mer peptides capable of inducing IFN-γ production. BALB/c mice were infected by the intranasal route with RSV wild-type strain A2 on day 0 and again on day 21. Splenocytes were isolated at day 8 (acute) or at day 48 (memory) after the second infection and stimulated in vitro in separate wells containing one of 46 overlapping peptides that were synthesized to represent the entire M2 protein from RSV strain A2. We utilized a panel of 15-mer peptides, overlapping by 11 amino acid, spanning the M2-1 protein, and numbered the peptides 1 through 46, based on their position relative to the N terminus of the protein. Splenocytes stimulated with individual peptides then were subjected to an IFN-γ ELISPOT assay. Since peptides 20 and 21 each contained the previously identified immunodominant CD8$^+$ T-lymphocyte epitope ($M2_{82-90}$), we expected high IFN-γ responses in response to these peptides. As expected, a robust response of 735 SFC per 10^6 splenocytes to peptide 20 was noted, and 810 SFC per 10^6 splenocytes responded to peptide 21, as shown in Fig. 1. These results suggested that RSV infection induced strong IFN-γ responses in the mice and that the ELISPOT assay was performing in an accurate manner. We found additional possible epitopes using the IFN-γ ELISPOT screening assay, since peptides 31, 32, and 45 induced low levels of reactivity during both the acute and memory phases of the experiment.

We analyzed the M2-1 predicted amino acid sequence for H-2^d-restricted CTL epitopes by using three different computer algorithms, namely, the RANKPEP, BIMAS, and SYFPEITHI epitope prediction programs (27–30). All prediction programs assigned top rankings to two nonamers, SYIG SINNI (amino acids 82 to 90) and VYNTVISYI (amino acids 127 to 135). While both BIMAS and SYFPEITHI predicted SYIGSINNI as number one and VYNTVISYI as number two, RANKPEP predicted VYNTVISYI as number one and SYIG SINNI as number two for the MHC class I allele. Peptides 20 and 21 contained SYIGSINNI and peptides 31 and 32 contained VYNTVISYI. The results from the ELISPOT assay and algorithm prediction programs suggested that the peptides 31 and 32 likely contain another epitope. Peptide 45 exhibited some possible reactivity in the ELISPOT assay, although the algorithm programs did not identify a sequence with the predicted binding motif.

Confirmation of ELISPOT results by flow cytometry. Since the ELISPOT assay did not distinguish CD4 from CD8 T lymphocyte responses, the splenocytes from day 48 postinfection (p.i.) also were tested by ICS for IFN-γ production after stimulation in vitro with peptide 20, 21, 31, 32, or 45. Influenza virus protein NP_{58-66} and the nonreactive RSV M2 peptide 36 were used as negative controls, and phorbol myristate acetate/ionomycin stimulation was used as a positive control for ICS. As shown in Fig. 2, the negative control groups stimulated with no peptide, influenza virus NP_{58-66}, or RSV M2 peptide 36, showed basal levels (0.10% to 0.13%) of IFN-γ production (Fig. 2A to C), while the positive control group using phorbol myristate acetate/ionomycin induced robust IFN-γ production to 20.3% (Fig. 2D). In the experimental groups, peptides 20 and 21 containing the dominant $M2_{82-90}$ epitope (SYIGSI NNI) stimulated IFN-γ production at 1.9% to 2.6% of CD8$^+$ T cells (Fig. 2E and F), while peptides 31 and 32 containing the predicted epitope VYNTVISYI induced 0.25% to 0.29% of

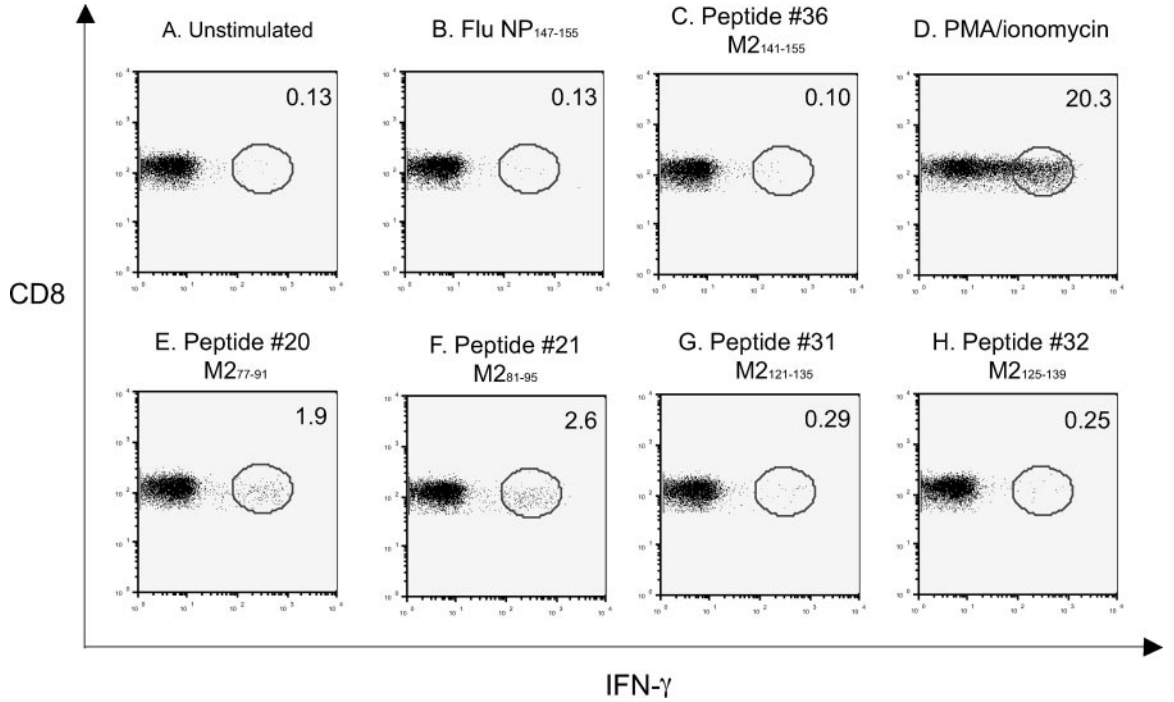

FIG. 2. Analysis of peptide-reactive $CD8^+$ T lymphocytes 48 days after a second infection. Splenocytes were incubated in the presence or absence of the peptides (1 μg/sample) in an intracellular cytokine staining assay for IFN-γ. The dot plots represent the production of IFN-γ from one of three representative experiments with similar results. Panels A to C show results for negative control stimulations. Flu $NP_{147-155}$, influenza virus protein $NP_{147-155}$. Panel D shows results for a positive control for maximal stimulation. Panels E and F show results for stimulations with $M2_{82-90}$. Panels G and H show results for stimulations with $M2_{127-135}$.

$CD8^+$ T cells to produce IFN-γ at day 48 p.i. (Fig. 2G and H). However, IFN-γ production was not detected in M2 peptide 45-stimulated animals despite numerous experiments (data not shown). Consequently, according to the results from the ELISPOT assay, algorithm prediction, and ICS experiments, we concluded that M2 peptides 31 and 32 contain a subdominant CTL epitope, since the immune response to this epitope was present but inferior in magnitude to that of $M2_{82-90}$.

Characterization of the optimal 9-mer epitope within the M2 peptides 31 and 32. To further define the optimal epitope in the M2 peptides 31 and 32, we synthesized eight truncated or mutated peptides representing this region (designated peptides A through I) and tested these peptides by monitoring the IFN-γ production by ELISPOT assay (Table 2). IFN-γ responses were determined at day 5 or day 12 p.i. in splenocytes. As shown in Fig. 3, panel A, splenocytes were unstimulated or

TABLE 2. Truncated peptide synthesis strategy to identify the optimal subdominant epitope within the $M2_{121-139}$ region

Category	Peptide[a]	Protein region (mutation)	Peptide sequence[b]
Control	36	$M2_{141-155}$	NNKQTIHLLKRLPAD
Subdominant M2 epitope	31	$M2_{121-135}$	NSPKIRV**Y**NTVISY**I**
	32	$M2_{125-139}$	IRV**Y**NYVISY**I**ESNR
	A	$M2_{125-135}$	IRV**Y**NTVISY**I**
	B	$M2_{121-134}$	IRV**Y**NTVISY
	C	$M2_{121-133}$	IRV**Y**NTVIS
	D	$M2_{121-132}$	IRV**Y**NTVI
	E	$M2_{126-135}$	RV**Y**NTVISY**I**
	F	$M2_{127-135}$	V**Y**NTVISY**I**
	G	$M2_{128-135}$	**Y**NTVISY**I**
	H	$M2_{127-135}$ (Y128R)	V***R***NTVISY**I**
Dominant M2 epitope	20	$M2_{77-91}$	VGVLES**Y**IGSINN**I**T
	21	$M2_{81-95}$	ES**Y**IGSINN**I**TKQSA
	I	$M2_{82-90}$	S**Y**IGSINN**I**

[a] The original 15-amino-acid peptides used for screening were numbered according to their relative positions from the N terminus (1 through 46). The truncated and variant peptides were assigned letter designations.

[b] The regions of peptides containing the optimal predicted nine-amino-acid epitope are underlined. Predicted anchor residues at position 2 or 9 are shown in bold. A mutated residue at position 2 is shown in italics.

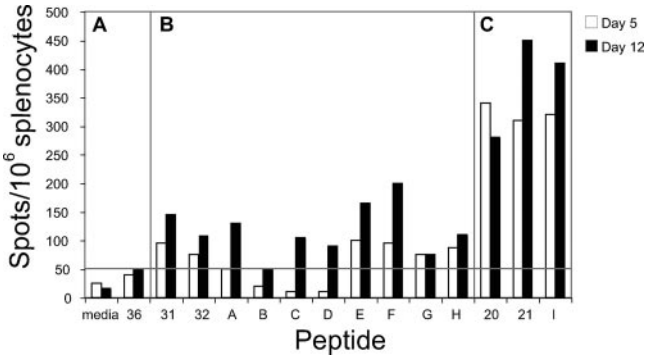

FIG. 3. Identification of the optimal epitope. IFN-γ responses were measured using truncated or mutated peptides. At day 5 (filled squares) or day 12 (open squares) after the second infection, animals were sacrificed and splenocytes were stimulated with the peptides indicated in Table 2. Data represent the results of an average of eight replicates. Group A, negative control medium or peptide; group B, truncated or mutated peptides for the subdominant epitope; group C, immunodominant epitope $M2_{82-90}$.

stimulated with peptide 36, panel B splenocytes were stimulated with the individual truncated peptides (Fig. 3, peptides A to G), anchor residue-mutated (Y128R) peptide (Fig. 3, peptide H), or peptides 31 and 32, and panel C splenocytes were stimulated with peptide 20 or 21 or the immunodominant $M2_{82-90}$ peptide (I) (Table 2 and Fig. 3). Since splenocytes stimulated with the peptide 36 at day 5 or day 12 produced from 20 to 40 SFC/10^6 splenocytes, we considered results of greater than 80 SFC at day 5 or greater than 100 SFC at day 12 to be positive signals. Group C splenocytes produced high numbers of IFN-γ SFC, which was expected, since this group received the immunodominant epitope. Peptide F contains the predicted optimal 9-mer ($M2_{127-135}$) of the subdominant epitope that was investigated in group B. As shown in Fig. 3, splenocytes stimulated with peptide F exhibited the most robust IFN-γ response at day 12 compared to the other truncated peptides in group B. Peptide H, mutated in the second residue that serves as an anchor residue (Y128R), elicited reduced IFN-γ responses. The other mutated epitopes exhibited reduced reactivity. Taken together, these results identified the optimal subdominant epitope as a 9-mer peptide, $M2_{127-135}$.

$M2_{127-135}$ represents a H-2K^d-restricted subdominant epitope. To determine whether the $M2_{127-135}$ peptide was K^d or L^d restricted, we tested the efficiency of $M2_{127-135}$ peptide binding to K^d or L^d by using an RMA-S cell line surface MHC stabilization assay. The RMA cell line does not express functional TAP-2 molecules. Its MHC class I molecules are thermolabile, and their surface expression level at 37°C is reduced significantly, due to the lack of high-affinity peptides normally transported from the cytosol. However, the MHC class I level is restored at 26°C or when high-affinity peptides are provided in a TAP-independent manner. The binding of such peptides can be monitored easily by determining the increase in the level of surface MHC class I. Interestingly, while the immunodominant $M2_{82-90}$ peptide bound to and stabilized K^d molecules to a high degree, the previously defined F_{85-93} K^d-restricted epitope stabilized K^d molecules poorly (Fig. 4B). The stabilization of the new subdominant epitope, $M2_{127-135}$, was intermediate between that of $M2_{82-90}$ and F_{85-93}. $M2_{127-135}$ and F_{85-93} lost their abilities to stabilize at a 10^{-8} M peptide concentration, but $M2_{82-90}$ lost stabilization at 10^{-10} M. In contrast, the three K^d-restricted epitopes used in this study, $M2_{82-90}$, $M2_{127-135}$, and F_{85-93}, did not bind to L^d molecules, as shown in Fig. 4A. These results clearly indicated that $M2_{127-135}$ is an H-2K^d-restricted epitope, exhibiting an intermediate affinity.

Conserved hierarchy of peptide-specific IFN-γ responses in systemic and local tissues. Since T-cell immune responses often differ in lymphoid (spleen) and nonlymphoid (lung) tissues, it was of interest to examine the level of RSV-specific T-cell responses in lymphoid compared to nonlymphoid tissues during an acute or memory phase (18, 25, 45). Thus, we measured the RSV M2-1 peptide-specific T-cell responses in the lungs and spleens of BALB/c mice after RSV infection. Splenocytes were isolated at different time points during acute (days 5 to 8), intermediate (days 13 to 35), or memory (days 42 to 60) phase following secondary infection. As shown in Fig. 5A, peptide 36-stimulated or unstimulated groups were considered negative controls. The basal levels of IFN-γ-producing T cells were 50 SFC/10^6 cells in acute phase, 45 SFC/10^6 cells in interme-

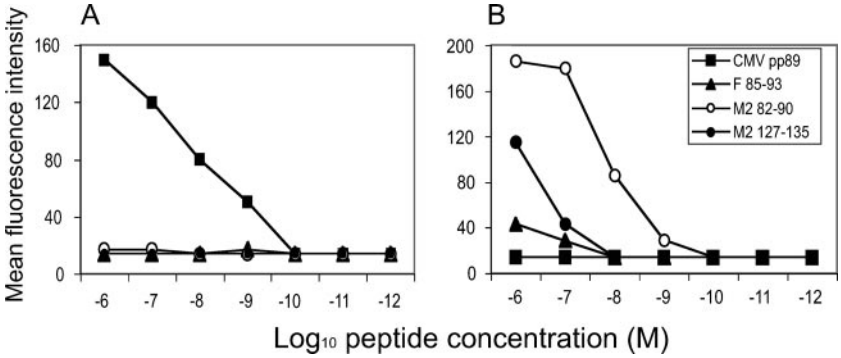

FIG. 4. Increased cell surface expression levels of H-2K^d MHC class I protein caused by $M2_{127-135}$. RMA-S cells expressing L^d (A) or K^d (B) molecules maintained at 26°C for 18 to 24 h were pulsed with increasing concentrations of the indicated peptides for 45 min at 26°C, washed, and incubated at 37°C for an additional 3 h. The RSV $M2_{82-90}$ SYIGSINNI peptide and RSV F_{85-93} KYKNAVTEL peptide were used as positive controls, and murine cytomegalovirus (CMV) pp89 YPHFMPTNL peptide was used as a negative control for K^d binding. For L^d binding, murine CMV pp89 peptide was used as the positive control and RSV $M2_{82-90}$ and RSV F_{85-93} were used as negative controls. Data represent the results from a single experiment, which was one of three with similar results.

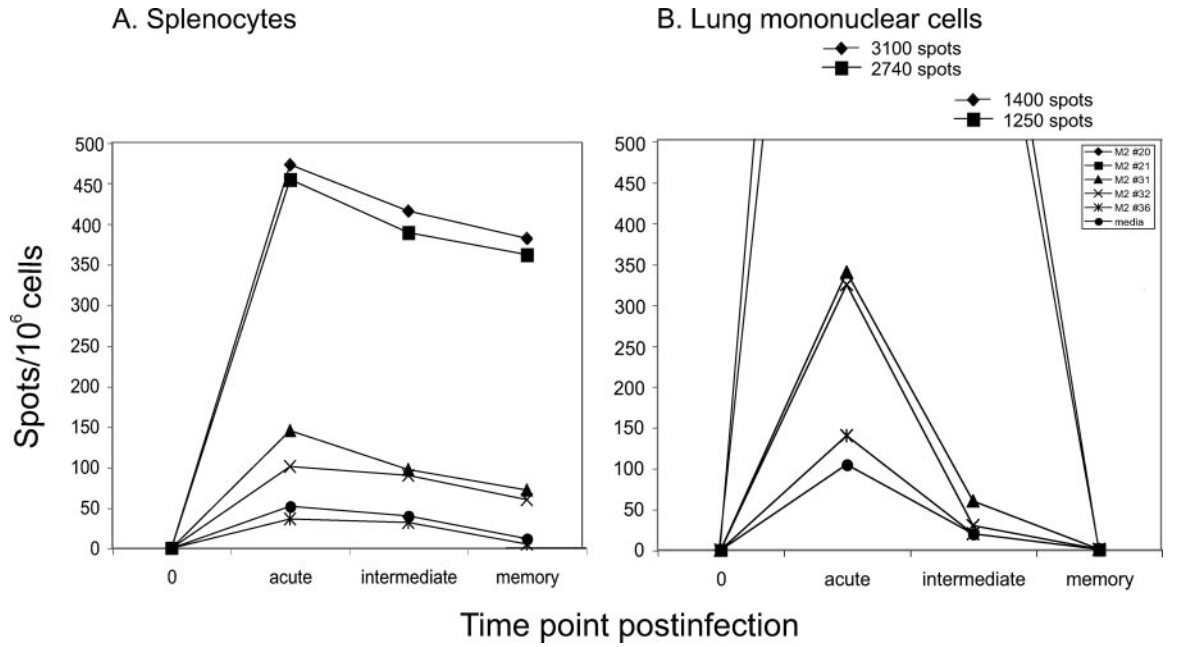

FIG. 5. Epitope hierarchy in the lung and spleen after the second RSV infection. Splenocytes (A) or lung lymphocytes (B) obtained at acute, intermediate, or memory phase after the second infection were restimulated in vitro with peptides and IFN-γ production was measured by using an ELISPOT assay. Data represent the averages from three independent experiments.

diate phase, and 10 SFC/10^6 cells in memory phase. For a negative control, we measured the spots in naïve mice. The level of IFN-γ-producing T cells in naïve mice was <1 SFC/10^6 cells at day 0. Peptides 31 and 32 containing the subdominant epitope elicited an IFN-γ ELISPOT response between 100 SFC/10^6 cells (acute) and 70 SFC/10^6 cells (memory). The ratio of SFC in negative controls to SFC in subdominant-epitope-stimulated groups was sustained at approximately 1:2 during acute, intermediate, and memory phases in the spleen.

Since T-cell immune responses could differ in lymphoid and nonlymphoid tissues, we compared spot numbers and kinetics of induction in the spleen and lung tissues. These ELISPOT ratios were in accordance with ratios determined by the IFN-γ ICS assay (Fig. 2). Lung lymphocytes also were isolated during acute, intermediate and memory phases. The pattern of IFN-γ production from subdominant epitope-specific T cells in the lung was very similar to that of the spleen. The ratio of negative control-stimulated group to subdominant epitope-stimulated groups in the lung was approximately 1:2 at the three different phases. Comparing the spot numbers and kinetics of induction in the two different tissues, we found that the numbers of IFN-γ-producing T cells were very high in the lung at acute phase compared to those in the spleen, consistent with the route of infection, which was direct inoculation of the respiratory tract (Fig. 5A and B). However, the relationship reversed during the memory phase, when the numbers of IFN-γ-producing T cells in the spleen were higher than those of the lung. The magnitude and kinetics of T-cell contraction differed in the two tissues, even though the pattern of hierarchy was similar in those tissues. In the immunodominant epitope (peptides 20 and 21)-stimulated groups, spot numbers of IFN-γ-producing T cells at acute phase dramatically reduced during the intermediate and memory phases in the lung, while the contraction of these cells in the spleen was much less dramatic.

Conserved hierarchy of epitope during primary and secondary RSV infection. Having identified a novel subdominant epitope during the early and memory phase of secondary infection as shown in Fig. 1 and 2, we sought to understand the evolution of the IFN-γ response to the dominant and subdominant epitopes following primary infection. BALB/c mice were infected with RSV wild-type strain A2 intranasally, and then splenocytes or lung lymphocytes were collected and stimulated with each of the 46 M2-1 peptides individually. Immune responses to the 46 overlapping peptides were monitored by IFN-γ ELISPOT analysis at day 10 or day 20 following primary infection. As shown in Fig. 6, splenocytes stimulated with peptide 20 or 21 (containing $M2_{82\text{-}90}$) exhibited robust IFN-γ responses at day 10 (Fig. 6C) or day 20 (Fig. 6D) after primary infection. This epitope appeared to be immunodominant during the early phase of acute infection, even though the numbers of IFN-γ SFC were low compared to those following secondary infection (Fig. 5A). Similar results were discovered in the lung at day 10 (Fig. 6A) and at day 20 (Fig. 6B). Interestingly, peptides 31 and 32 stimulated splenocytes to produce IFN-γ-specific spots at day 10 (11 to 17 SFC/10^6 cells) and at day 20 (6 SFC/10^6 cells). The number of SFC induced by these peptides was very similar in the lung (Fig. 6A) and in the spleen (Fig. 6C) after primary infection. The pattern of subdominance for the epitope in peptides 31 and 32 was more significant in the lung than in the spleen. The data suggest that the pattern of dominance and subdominance for $M2_{82\text{-}90}$ and $M2_{127\text{-}135}$ was conserved in primary and secondary infection, but was regulated in a tissue-specific fashion.

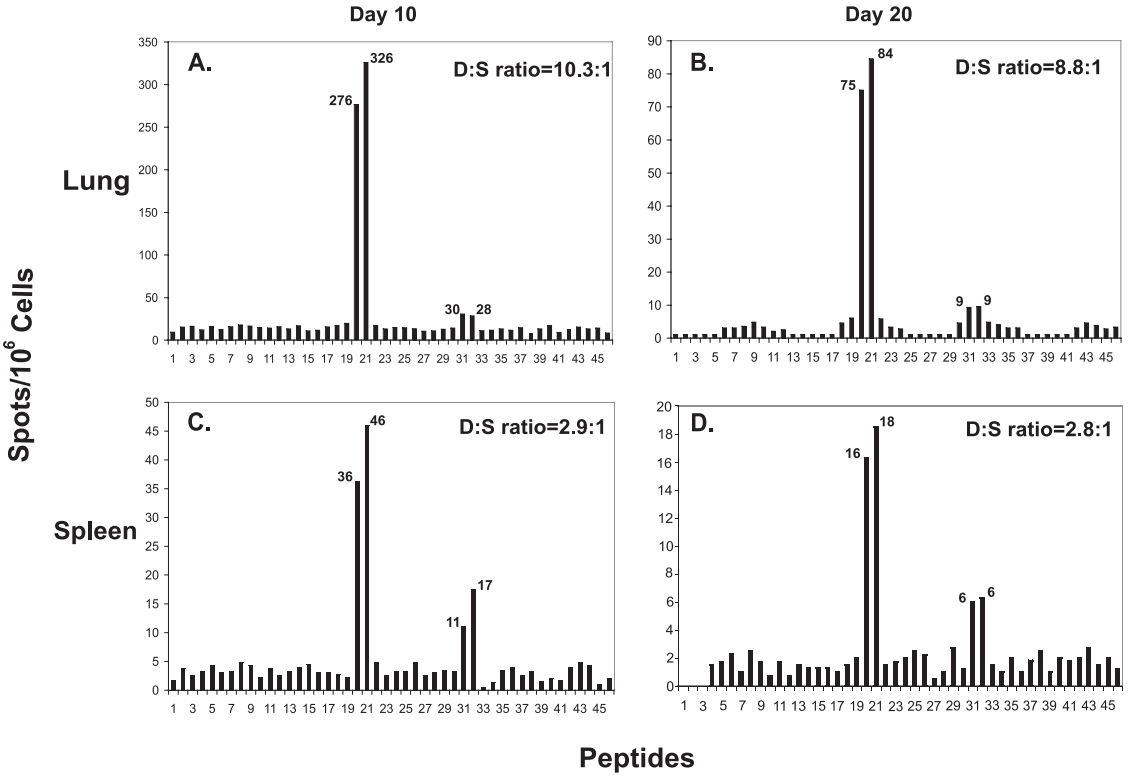

FIG. 6. Epitope hierarchy in the lung and spleen after RSV primary infection. Lung lymphocytes isolated at day 10 (A) or day 20 (B) or splenocytes isolated at day 10 (C) or day 20 (D) after primary infection were restimulated with a panel of peptides and IFN-γ production was measured using the ELISPOT assay. The average number of spots is indicated at the peak of each bar for the dominant and subdominant epitopes. The dominant/subdominant (D:S) ratio is the ratio of the mean number of spots of peptides 20 and 21 to that of peptides 31 and 32.

$M2_{82-90}$ and $M2_{127-135}$ epitope-specific $CD8^+$ T-lymphocyte responses in splenocytes. Epitope-specific CTL responses were monitored by quantitating MHC/peptide tetramer binding $CD8^+$ T lymphocytes following infection. Mice were infected by the intranasal route with RSV wild-type strain A2 on day 0 and again on day 21. Splenocytes or lung lymphocytes were isolated at day 8 after the second infection and the frequencies of RSV-specific $CD8^+$ T lymphocytes were analyzed using K^d MHC class I tetramers containing the $M2_{82-90}$ peptide or the $M2_{127-135}$ peptide. Freshly isolated splenocytes or lung lymphocytes were stained for surface CD3 and CD8 and the indicated tetramer. Among $CD3^+/CD8^+$ gated splenocytes, 1.1% of cells stained with the H-2K^d/$M2_{82-90}$ tetramer, as shown in Fig. 7E. In contrast, $M2_{127-135}$ tetramer-positive cells were 0.3% of $CD8^+$ splenocytes (Fig. 7F). Nonspecific binding of the tetramers using naïve splenocytes in this assay was very low (Fig. 7A, B, and C). In lung lymphocytes, 62% of cells were stained with the H-2K^d/$M2_{82-90}$ tetramer (Fig. 8A) and 6.1% of cells were stained with the H-2K^d/$M2_{127-135}$ tetramer (Fig. 8C). The numbers of T lymphocytes stained with the K^d tetramers containing RSV M2 epitopes correlated highly with the frequencies determined by ELISPOT assay, shown in Fig. 1 and 5. Interestingly, the ratio of T lymphocytes specific for $M2_{82-90}$ or $M2_{127-135}$ was approximately 3:1 in spleen, and 10:1 in lung lymphocytes. These ratios in both tissues also were consistent with the results in the ELISPOT assay and revealed a tissue-specific regulation of immunodominance.

DISCUSSION

$CD8^+$ T lymphocytes play an important role in clearance of virus and recovery from RSV infection in both humans and in the murine model. A striking feature of the CTL response to a protein antigen in mice is the limited number of epitopes recognized by the CTLs in association with an MHC class I molecule (9). Pathogens elicit diverse T-lymphocyte responses that have been categorized as dominant or subdominant, thereby establishing an immunodominance hierarchy. It is important to identify MHC class I-restricted CTL epitopes in order to examine cellular immune responses to infection and understand the mechanisms that regulate dominance hierarchies. In this report, we identified a new subdominant K^d-restricted CTL epitope for BALB/c mice within the RSV M2 protein, $M2_{127-135}$. Furthermore, we measured the kinetics and expansion of $M2_{127-135}$-specific $CD8^+$ T lymphocytes in the spleen or lung following primary or secondary infection by ELISPOT assay, ICS, and tetramer staining and compared this response to that of a dominant epitope in the same viral protein. We also detected reactivity in ELISPOT screening assays to a region in M2-1 represented by peptide 45. However, this synthetic peptide did not induce detectable reactivity above background in ICS assays and does not contain a predicted H-2K^d binding motif, suggesting it does not contain a bona fide MHC class I restricted CD8 T-cell epitope.

It is well known that MHC class I molecules are capable of

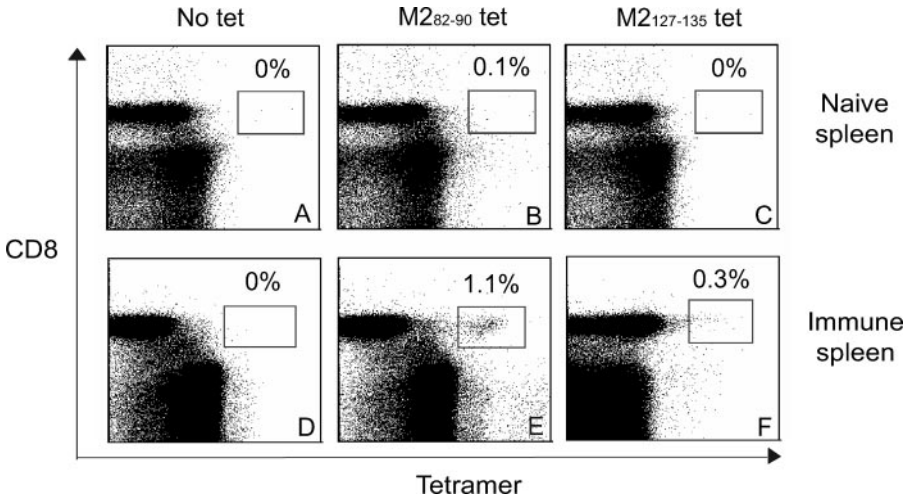

FIG. 7. Direct enumeration of $M2_{82-90}$ or $M2_{127-135}$ epitope-specific $CD8^+$ T lymphocytes. Groups of BALB/c mice were infected twice with RSV wild-type strain A2. Splenocytes (D, E, and F) were harvested 8 days following the second infection and tested by flow cytometric analysis after staining with the $M2_{82-90}$ tetramer (B and E) or $M2_{127-135}$ tetramer (C and F). Splenocytes from naïve mice were used as negative controls (A, B, and C). Dot plots illustrate results for total $CD3^+$ lymphocytes as well as 50,000 $CD8^+$ T lymphocytes. Numbers shown in the rectangular gate correspond to the percentage of $CD8^+$ lymphocytes stained by the respective tetramer (tet). Data represent the results of a single experiment, which was one of five with similar results.

binding diverse peptides. These peptides are generally 8 to 10 amino acids in length, and both N and C termini are bound by hydrogen bonds to the peptide binding cleft in class I molecules. In general, two side-chains, one at the amino terminus (usually at position 2) and the other at the carboxyl terminus (usually at position 9), hold the peptide in the allele-specific pocket. In this study, we used three separate computer algorithms, SYFPEITHI, BIMAS, and RANKPEP to identify putative epitopes in larger peptides that exhibited biologic activity. These algorithms predict putative CTL epitopes in protein sequences by identifying peptides that contain the anchor motifs optimal for binding to particular MHC molecules. These algorithms have limitations. Since algorithms are based on the peptides identified experimentally to date, they are descriptive of the most common motifs observed in past experiments. Even though algorithm prediction is not perfect, all three algorithms predicted the new subdominant epitope correctly.

Little is known about the molecular determinants of immunodominance or how immunodominant and subdominant determinants are distinguished by the TCR repertoire. The underlying mechanisms of dominance and subdominance are complex, since all aspects of $CD8^+$ T lymphocytes biology are involved in this process, including (i) positive and negative selection of the TCR repertoire in the thymus and periphery, (ii) interaction of $CD8^+$ T lymphocytes with professional antigen-presenting cells, (iii) T-lymphocyte priming and expansion, (iv) short peptide generation via the proteasome, (v) TAP-dependent or -independent transport of peptide into the ER, (vi) peptide binding affinity to MHC class I molecules, and (vii) antigenic competition. Understanding immunodominance could be very useful for manipulating and determining the cellular immune response to respiratory pathogens, including RSV, especially during the development of candidate vaccines. In this study, we tested the peptide binding affinities of $M2_{82-90}$ and $M2_{127-135}$ to K^d and L^d molecules. The BIMAS algorithm

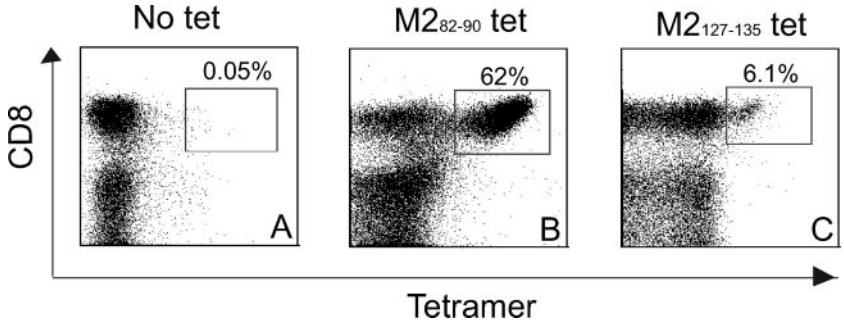

FIG. 8. Direct enumeration of $M2_{82-90}$ or $M2_{127-135}$ epitope-specific $CD8^+$ T lymphocytes. Groups of BALB/c mice were infected twice with RSV wild-type strain A2. Lung lymphocytes (A, B, and C) were harvested 8 days following the second infection and tested by flow cytometric analysis after staining with no tetramer (A), $M2_{82-90}$ tetramer (B), or $M2_{127-135}$ tetramer (C). Dot plots illustrate results for total $CD3^+$ lymphocytes as well as 20,000 $CD8^+$ T lymphocytes. Numbers shown in the rectangular gate correspond to the percentages of $CD8^+$ lymphocytes stained by the respective tetramers (tet). Data shown are representative of five experiments.

predicted the estimated scores for half-time of dissociation from H-2K^d to be 5,760 for $M2_{82-90}$, 3,456 for F_{85-93}, and 2,400 for $M2_{127-135}$. However, we found experimentally that the $M2_{127-135}$ peptide bound to K^d molecules more efficiently than the previously described epitope F_{85-93} in the RMA-S–K^d stabilization assay. These data suggest that the weak functional responses to $M2_{127-135}$ were not simply due to insufficient binding affinity for K^d molecules.

There are several studies that show that the specificities of CTL responses to antigen can differ between primary and secondary infections in influenza virus model systems (4, 10, 13). Here, we investigated the reversal of the epitope hierarchy in primary and secondary RSV infections. Unlike for influenza virus, a strict maintenance of epitope hierarchy in primary and secondary infection was observed in our RSV model. The control of immunodominance hierarchies in responses to viral epitopes is of interest. For instance, immunodominance has been investigated in the well-characterized mouse models for infections with lymphocytic choriomeningitis virus (38, 39) and influenza virus (5, 13) among viral pathogens and in *Listeria monocytogenes* infection (16, 44). Although the immunodominant RSV CTL epitope $M2_{82-90}$ was discovered over a decade ago, the number of epitopes available for study of immunodominance in the response to RSV was limited. To date, five RSV-specific epitopes in BALB/c mice have been identified and one in C57BL/6 mice has been discovered. Four H-2^d CTL epitopes, $M2_{82-90}$ (21, 22), F_{85-93} (8), and F_{92-106} (19) were identified following RSV strain A2 infection and $F_{249-258}$ (20) was identified following RSV Long strain infection. The $M2_{82-90}$ epitope appears immunodominant compared to the other identified epitopes in BALB/c mice. One other epitope identified in BALB/c mice was $G_{183-197}$, an I-E^d-restricted CD4$^+$ T-lymphocyte epitope (41). We also identified an H-2D^b-restricted CTL epitope in the M protein (36). This epitope is the only RSV epitope identified to date for C57BL/6 mice. A study similar to our current work was published based on a recently discovered epitope $M_{187-195}$ in C57BL/6 (H-2^b) mouse model (24). In this work, the investigators characterized CD8$^+$ T cells during primary and secondary infection in lung and spleen of C57BL/6 mice and found M epitope-specific reactivity in both primary and secondary responses.

Since the tissue distribution of T cells may affect immunodominance (18, 24, 44), we investigated the frequencies of epitope-specific T cells in different tissues. Marshall et al. (25) measured influenza virus-specific CD8$^+$ T cells in different tissues, such as the spleen, lung, nasal mucosa-associated lymphoid tissue, and liver, as well as in blood, by using a tetramer-staining technique. They found evidence for an altered pattern of immunodominance of epitopes in different tissues. Wherry et al. investigated the relationship between epitope specificity and tissue distribution in the lymphocytic choriomeningitis virus mouse model (45), and Huleatt et al. tested this concept in the mouse model of *Listeria* infection (18). Each of those three studies used epitopes in two different proteins to investigate the relationship between epitope hierarchy and tissue distribution. Differing levels of expression of two proteins in tissues could affect epitope hierarchies. Our new model avoids this issue by studying two epitopes in the same protein and thus should serve as an ideal model for further study of the immune factors affecting epitope hierarchy.

The epitope hierarchy in RSV has been poorly investigated because of the limited number of epitopes, especially epitopes within a single protein. In consequence, our discovery of a new subdominant epitope, $M2_{127-135}$, in the same protein as the dominant epitope for the virus in BALB/c mice provides an optimal tool for studies of epitope hierarchy in RSV infection. Interestingly, the kinetics and ratios of induction of $M2_{82-90}$- and $M2_{127-135}$-specific T lymphocytes was highly regulated in both the acute (day 8 p.i.) and memory (day 48 p.i.) phases, and the results from the ELISPOT assay and tetramer staining correlated highly. The ratios of dominant epitope reactivity to subdominant epitope reactivity differed in the local and systemic tissues, suggesting tissue-specific regulatory mechanisms.

Further characterization and understanding of the control of RSV CD8$^+$ T-cell epitope immunodominance hierarchies will facilitate the rational development of new vaccine candidates.

ACKNOWLEDGMENTS

This work was supported in part by a grant from the NIAID, R01 AI-53222.

We thank E. Pamer for providing RMA-S cells expressing K^d and T. Hansen for providing RMA-S cells expressing L^d.

REFERENCES

1. **Andreansky, S. S., J. Stambas, P. G. Thomas, W. Xie, R. J. Webby, and P. C. Doherty.** 2005. Consequences of immunodominant epitope deletion for minor influenza virus-specific CD8$^+$-T-cell responses. J. Virol. **79:**4329–4339.
2. **Anthony, D. D., and P. V. Lehmann.** 2003. T-cell epitope mapping using the ELISPOT approach. Methods **29:**260–269.
3. **Bangham, C. R., P. J. Openshaw, L. A. Ball, A. M. King, G. W. Wertz, and B. A. Askonas.** 1986. Human and murine cytotoxic T cells specific to respiratory syncytial virus recognize the viral nucleoprotein (N), but not the major glycoprotein (G), expressed by vaccinia virus recombinants. J. Immunol. **137:**3973–3977.
4. **Belz, G. T., W. Xie, J. D. Altman, and P. C. Doherty.** 2000. A previously unrecognized H-2D^b-restricted peptide prominent in the primary influenza A virus-specific CD8$^+$ T-cell response is much less apparent following secondary challenge. J. Virol. **74:**3486–3493.
5. **Belz, G. T., W. Xie, and P. C. Doherty.** 2001. Diversity of epitope and cytokine profiles for primary and secondary influenza A virus-specific CD8+ T cell responses. J. Immunol. **166:**4627–4633.
6. **Brock, S. C., J. M. Heck, P. A. McGraw, and J. E. Crowe, Jr.** 2005. The transmembrane domain of the respiratory syncytial virus F protein is an orientation-independent apical plasma membrane sorting sequence. J. Virol. **79:**12528–12535.
7. **Busch, D. H., and E. G. Pamer.** 1998. MHC class I/peptide stability: implications for immunodominance, in vitro proliferation, and diversity of responding CTL. J. Immunol. **160:**4441–4448.
8. **Chang, J., A. Srikiatkhachorn, and T. J. Braciale.** 2001. Visualization and characterization of respiratory syncytial virus F-specific CD8(+) T cells during experimental virus infection. J. Immunol. **167:**4254–4260.
9. **Chen, W., L. C. Anton, J. R. Bennink, and J. W. Yewdell.** 2000. Dissecting the multifactorial causes of immunodominance in class I-restricted T cell responses to viruses. Immunity **12:**83–93.
10. **Chen, W., K. Pang, K. A. Masterman, G. Kennedy, S. Basta, N. Dimopoulos, F. Hornung, M. Smyth, J. R. Bennink, and J. W. Yewdell.** 2004. Reversal in the immunodominance hierarchy in secondary CD8+ T cell responses to influenza A virus: roles for cross-presentation and lysis-independent immunodomination. J. Immunol. **173:**5021–5027.
11. **Cherrie, A. H., K. Anderson, G. W. Wertz, and P. J. Openshaw.** 1992. Human cytotoxic T cells stimulated by antigen on dendritic cells recognize the N, SH, F, M, 22K, and 1b proteins of respiratory syncytial virus. J. Virol. **66:**2102–2110.
12. **Crowe, J. E., Jr.** 2001. Respiratory syncytial virus vaccine development. Vaccine **20**(Suppl. 1)**:**S32–S37.
13. **Crowe, S. R., S. J. Turner, S. C. Miller, A. D. Roberts, R. A. Rappolo, P. C. Doherty, K. H. Ely, and D. L. Woodland.** 2003. Differential antigen presentation regulates the changing patterns of CD8+ T cell immunodominance in primary and secondary influenza virus infections. J. Exp. Med. **198:**399–410.
14. **Dudas, R. A., and R. A. Karron.** 1998. Respiratory syncytial virus vaccines. Clin. Microbiol. Rev. **11:**430–439.
15. **Everard, M. L.** 2006. The role of the respiratory syncytial virus in airway syndromes in childhood. Curr. Allergy Asthma Rep. **6:**97–102.
16. **Finelli, A., K. M. Kerksiek, S. E. Allen, N. Marshall, R. Mercado, I. Pilip,**

D. H. Busch, and E. G. Pamer. 1999. MHC class I restricted T cell responses to Listeria monocytogenes, an intracellular bacterial pathogen. Immunol. Res. **19:**211–223.
17. **Graham, B. S., L. A. Bunton, P. F. Wright, and D. T. Karzon.** 1991. Role of T lymphocyte subsets in the pathogenesis of primary infection and rechallenge with respiratory syncytial virus in mice. J. Clin. Investig. **88:**1026–1033.
18. **Huleatt, J. W., I. Pilip, K. Kerksiek, and E. G. Pamer.** 2001. Intestinal and splenic T cell responses to enteric Listeria monocytogenes infection: distinct repertoires of responding CD8 T lymphocytes. J. Immunol. **166:**4065–4073.
19. **Jiang, S., N. J. Borthwick, P. Morrison, G. F. Gao, and M. W. Steward.** 2002. Virus-specific CTL responses induced by an H-2K(d)-restricted, motif-negative 15-mer peptide from the fusion protein of respiratory syncytial virus. J Gen. Virol. **83:**429–438.
20. **Johnstone, C., P. de Leon, F. Medina, J. A. Melero, B. Garcia-Barreno, and M. Del Val.** 2004. Shifting immunodominance pattern of two cytotoxic T-lymphocyte epitopes in the F glycoprotein of the Long strain of respiratory syncytial virus. J. Gen. Virol. **85:**3229–3238.
21. **Kulkarni, A. B., P. L. Collins, I. Bacik, J. W. Yewdell, J. R. Bennink, J. E. Crowe, Jr., and B. R. Murphy.** 1995. Cytotoxic T cells specific for a single peptide on the M2 protein of respiratory syncytial virus are the sole mediators of resistance induced by immunization with M2 encoded by a recombinant vaccinia virus. J. Virol. **69:**1261–1264.
22. **Kulkarni, A. B., M. Connors, C. Y. Firestone, H. C. Morse III, and B. R. Murphy.** 1993. The cytolytic activity of pulmonary $CD8^+$ lymphocytes, induced by infection with a vaccinia virus recombinant expressing the M2 protein of respiratory syncytial virus (RSV), correlates with resistance to RSV infection in mice. J. Virol. **67:**1044–1049.
23. **La Gruta, N. L., K. Kedzierska, K. Pang, R. Webby, M. Davenport, W. Chen, S. J. Turner, and P. C. Doherty.** 2006. A virus-specific CD8+ T cell immunodominance hierarchy determined by antigen dose and precursor frequencies. Proc. Natl. Acad. Sci. USA **103:**994–999.
24. **Lukens, M. V., E. A. Claassen, P. M. de Graaff, M. E. van Dijk, P. Hoogerhout, M. Toebes, T. N. Schumacher, R. G. van der Most, J. L. Kimpen, and G. M. van Bleek.** 2006. Characterization of the CD8+ T cell responses directed against respiratory syncytial virus during primary and secondary infection in C57BL/6 mice. Virology **352:**157–168.
25. **Marshall, D. R., S. J. Turner, G. T. Belz, S. Wingo, S. Andreansky, M. Y. Sangster, J. M. Riberdy, T. Liu, M. Tan, and P. C. Doherty.** 2001. Measuring the diaspora for virus-specific CD8+ T cells. Proc. Natl. Acad. Sci. USA **98:**6313–6318.
26. **Meierhoff, G., P. A. Ott, P. V. Lehmann, and N. C. Schloot.** 2002. Cytokine detection by ELISPOT: relevance for immunological studies in type 1 diabetes. Diabetes Metab. Res. Rev. **18:**367–380.
27. **Murali-Krishna, K., J. D. Altman, M. Suresh, D. J. Sourdive, A. J. Zajac, J. D. Miller, J. Slansky, and R. Ahmed.** 1998. Counting antigen-specific CD8 T cells: a reevaluation of bystander activation during viral infection. Immunity **8:**177–187.
27a. **National Research Council.** 1996. Guide for the care and use of laboratory animals. National Academy Press, Washington, DC.
28. **Nicholson, K. G., T. McNally, M. Silverman, P. Simons, J. D. Stockton, and M. C. Zambon.** 2006. Rates of hospitalisation for influenza, respiratory syncytial virus and human metapneumovirus among infants and young children. Vaccine **24:**102–108.
29. **Openshaw, P. J., K. Anderson, G. W. Wertz, and B. A. Askonas.** 1990. The 22,000-kilodalton protein of respiratory syncytial virus is a major target for K^d-restricted cytotoxic T lymphocytes from mice primed by infection. J. Virol. **64:**1683–1689.
30. **Parker, K. C., M. A. Bednarek, and J. E. Coligan.** 1994. Scheme for ranking potential HLA-A2 binding peptides based on independent binding of individual peptide side-chains. J. Immunol. **152:**163–175.
31. **Rammensee, H., J. Bachmann, N. P. Emmerich, O. A. Bachor, and S. Stevanovic.** 1999. SYFPEITHI: database for MHC ligands and peptide motifs. Immunogenetics **50:**213–219.
32. **Reche, P. A., J. P. Glutting, and E. L. Reinherz.** 2002. Prediction of MHC class I binding peptides using profile motifs. Hum.Immunol. **63:**701–709.
33. **Reche, P. A., J. P. Glutting, H. Zhang, and E. L. Reinherz.** 2004. Enhancement to the RANKPEP resource for the prediction of peptide binding to MHC molecules using profiles. Immunogenetics **56:**405–419.
34. **Rock, M. T., and J. E. Crowe, Jr.** 2003. Identification of a novel human leucocyte antigen-A*01-restricted cytotoxic T-lymphocyte epitope in the respiratory syncytial virus fusion protein. Immunology **108:**474–480.
35. **Rodriguez, F., S. Harkins, M. K. Slifka, and J. L. Whitton.** 2002. Immunodominance in virus-induced $CD8^+$ T-cell responses is dramatically modified by DNA immunization and is regulated by gamma interferon. J. Virol. **76:**4251–4259.
36. **Rutigliano, J. A., M. T. Rock, A. K. Johnson, J. E. Crowe, Jr., and B. S. Graham.** 2005. Identification of an H-2D(b)-restricted CD8+ cytotoxic T lymphocyte epitope in the matrix protein of respiratory syncytial virus. Virology **337:**335–343.
37. **Sijts, A. J., A. Neisig, J. Neefjes, and E. G. Pamer.** 1996. Two Listeria monocytogenes CTL epitopes are processed from the same antigen with different efficiencies. J. Immunol. **156:**683–692.
38. **Slifka, M. K., J. N. Blattman, D. J. Sourdive, F. Liu, D. L. Huffman, T. Wolfe, A. Hughes, M. B. Oldstone, R. Ahmed, and M. G. Von Herrath.** 2003. Preferential escape of subdominant CD8+ T cells during negative selection results in an altered antiviral T cell hierarchy. J. Immunol. **170:**1231–1239.
39. **van der Most, R. G., K. Murali-Krishna, J. G. Lanier, E. J. Wherry, M. T. Puglielli, J. N. Blattman, A. Sette, and R. Ahmed.** 2003. Changing immunodominance patterns in antiviral CD8 T-cell responses after loss of epitope presentation or chronic antigenic stimulation. Virology **315:**93–102.
40. **van der Most, R. G., K. Murali-Krishna, J. L. Whitton, C. Oseroff, J. Alexander, S. Southwood, J. Sidney, R. W. Chesnut, A. Sette, and R. Ahmed.** 1998. Identification of Db- and Kb-restricted subdominant cytotoxic T-cell responses in lymphocytic choriomeningitis virus-infected mice. Virology **240:**158–167.
41. **Varga, S. M., E. L. Wissinger, and T. J. Braciale.** 2000. The attachment (G) glycoprotein of respiratory syncytial virus contains a single immunodominant epitope that elicits both Th1 and Th2 CD4+ T cell responses. J. Immunol. **165:**6487–6495.
42. **Venter, M., M. Rock, A. J. Puren, C. T. Tiemessen, and J. E. Crowe, Jr.** 2003. Respiratory syncytial virus nucleoprotein-specific cytotoxic T-cell epitopes in a South African population of diverse HLA types are conserved in circulating field strains. J. Virol. **77:**7319–7329.
43. **Vijh, S., and E. G. Pamer.** 1997. Immunodominant and subdominant CTL responses to Listeria monocytogenes infection. J. Immunol. **158:**3366–3371.
44. **Vijh, S., I. M. Pilip, and E. G. Pamer.** 1999. Noncompetitive expansion of cytotoxic T lymphocytes specific for different antigens during bacterial infection. Infect. Immun. **67:**1303–1309.
45. **Wherry, E. J., J. N. Blattman, K. Murali-Krishna, R. van der Most, and R. Ahmed.** 2003. Viral persistence alters CD8 T-cell immunodominance and tissue distribution and results in distinct stages of functional impairment. J. Virol. **77:**4911–4927.
46. **Yewdell, J. W., and M. Del Val.** 2004. Immunodominance in TCD8+ responses to viruses: cell biology, cellular immunology, and mathematical models. Immunity **21:**149–153.